



PERGAMON

Solid-State Electronics xxx (2002) xxx-xxx

SOLID-STATE  
ELECTRONICS

www.elsevier.com/locate/sse

# A method to evaluate the location of the maximum value of a function with high level of noise

A. Ortiz-Conde <sup>a,\*</sup>, F.J. García Sánchez <sup>a</sup>, A. Caralli D'Ambrosio <sup>b</sup>

<sup>a</sup> Laboratorio de Electrónica del Estado Sólido (LEES), Universidad Simón Bolívar, Apartado Postal 89000, Caracas 1080A, Venezuela

<sup>b</sup> Universidad de Carabobo, Valencia, Carabobo, Venezuela

Received 1 May 2002; received in revised form 2 June 2002; accepted 19 June 2002

## Abstract

This note presents a new method that evaluates the location of the maximum value of a given function under the presence of high level of noise. Because the method is based on integration rather than on differentiation, it decreases the effect of noise instead of increasing it. The method's effectiveness is verified by determining the gate voltage corresponding to the maximum slope of simulated and experimental MOSFET transconductance characteristics.

© 2002 Published by Elsevier Science Ltd.

**Keywords:** Parameter extraction; Maximum location; Potential functions; Experimental noise

## 1. Introduction

There are many applications, such as parameter extraction methods for semiconductor device models [1-6], which require the evaluation of the location of a maximum value of a given function  $y(x)$ . The usual mathematical approach to evaluate this value  $x_{max}$ , corresponding to the maximum value of the function,  $y_{max}$ , consists on finding the derivative  $dy/dx$  and then solving  $dy/dx = 0$ . However, such procedure is not recommendable for noisy data because the derivative worsens the effect of experimental noise [7-9].

The present method, which is based on integration, evaluates the location of the maximum even in the presence of high level of noise. AIM-SPICE [10] simulation results, with and without added noise, as well as actual measured data will be used to test this extraction method.

## 2. Foundation of the method

Let  $y(x)$  be a continuous function with a maximum  $y_{max}$  at  $x = x_{max}$ . Then the Content function is given by [7,8,11]

$$C(x, y) \equiv \int_0^y x dy, \tag{1}$$

represents the area contained between the function and the vertical axis. Using integration by parts  $C$  can be expressed as:

$$C(x, y) = xy - \int_0^x y dx, \tag{2}$$

where the second term in the right-hand side of (2) is known as the Co-Content [11].

For the function considered, the Content increases up to  $x = x_{max}$  as  $y$  and  $x$  both increase. Above  $x = x_{max}$  the Content decreases as  $y$  decreases and  $x$  increases. Therefore, the Content exhibits a maximum at  $x = x_{max}$ , as may be also easily seen by taking the derivative of  $C$  in (2):

$$\frac{dC}{dx} \equiv y - x \frac{dy}{dx} - y = -x \frac{dy}{dx}, \tag{3}$$

\* Corresponding author. Fax: +58-2-9063631.

E-mail addresses: [ortizc@ieec.org](mailto:ortizc@ieec.org) (A. Ortiz-Conde), [acaralli@ieec.org](mailto:acaralli@ieec.org) (A. Caralli D'Ambrosio).

51 and observing that  $dC/dx = 0$  at  $x = x_{\max}$  because  
52  $dy/dx = 0$ .

53 Therefore a plot of the Content versus  $y$  is a double-  
54 value function which presents a peak at  $y = y_{\max}$  corre-  
55 sponding to the value  $x = x_{\max}$  (see Fig. 3). The slope at  
56 this peak yields the value of  $x_{\max}$  since  $dC/dy \equiv x$ .

57 It is worth noting that the Content is just a particular  
58 case (for  $p = 0$ ) of the family of potential functions de-  
59 fined by [7]:

$$F_p(x, y) \equiv x \cdot y - (p + 1) \int_0^x y dx. \quad (4)$$

61 We have previously used the case of  $p = 1$  to measure  
62 distortion [9] and for parameter extraction [2-4,6,8].

63 As an illustrative example we will study the second-  
64 derivative method [5] to extract the threshold voltage  
65 ( $V_T$ ) of a MOSFET. This method [5] was developed to  
66 avoid the effects of the parasitic drain/source series re-  
67 sistances. It determines  $V_T$  as the gate voltage at which  
68 the derivative of the transconductance (i.e.,  
69  $K = dg_m/dV_g = d^2I_D/dV_g^2$ ) is maximum. We selected this  
70  $V_T$  extraction method because it takes the second-deri-  
71 vative of the measured data and it is therefore highly  
72 sensitive to any measurement noise that might be pres-  
73 sent.

### 74 3. Application to simulated characteristics without noise

75 The new extraction procedure was firstly applied to  
76 AIM-SPICE [10] simulation results for a short-channel  
77 MOSFET. The parameters used are: level = 8, a  
78 threshold voltage of 0.5 V, a channel width of 5  $\mu\text{m}$ ,  
79 mask channel length of 0.18  $\mu\text{m}$ , front gate oxide  
80 thickness of 3.2 nm, a doping density of  $1 \times 10^{18} \text{ cm}^{-3}$ , a  
81 low-field mobility of 500  $\text{cm}^2/\text{Vs}$ , and zero lateral dif-  
82 fusion. For simplicity, in the present work a zero mo-  
83 bility degradation coefficient, a very high saturation  
84 velocity of  $6 \times 10^8 \text{ cm/s}$  and a drain/source series re-  
85 sistance of 37.51  $\Omega$  were selected to approximately fit the  
86 simulated to the experimental data that will be presented  
87 in Section 5. The drain/source series resistances were  
88 defined externally to the device with the model's internal  
89 parasitic resistance set to zero. Previous work [12] has  
90 shown that the mobility degradation effect and the sat-  
91 uration velocity can be modeled in the  $I_D$ - $V_g$  charac-  
92 teristics as an effective resistance in series with the drain/  
93 source resistance.

94 Fig. 1(a) shows the  $I_D$  versus  $V_g$  characteristics without  
95 added noise simulated at  $V_d = 10 \text{ mV}$  with increments of  
96 10 mV. Fig. 1(b) presents the resulting transconductance  
97 as calculated from:  $g_m \equiv dI_D/dV_g$ . Here the variable  $V_g$   
98 corresponds to the variable  $x$  defined in Section 2.

99 Fig. 2(a) illustrates the simulated  $K$ - $V_g$  characteristics  
100 obtained from  $K \equiv dg_m/dV_g \equiv d^2I_D/dV_g^2$  for this noise-

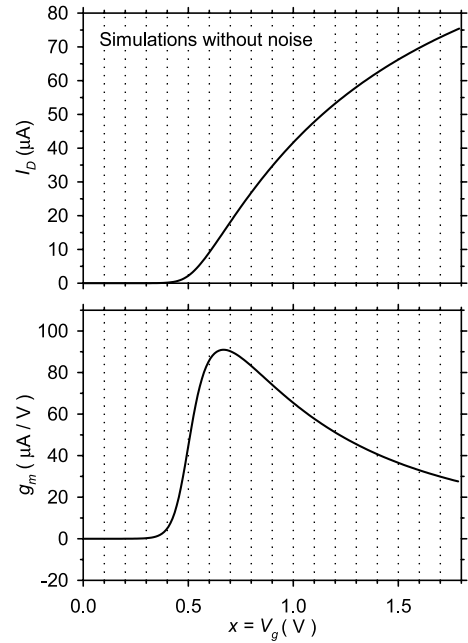


Fig. 1. (a) Simulated  $I_D$ - $V_g$  transfer characteristics at  $V_d = 10 \text{ mV}$  with increments of 10 mV without experimental noise; and (b) resulting transconductance obtained from  $g_m = dI_D/dV_g$ . The variable  $V_g$  corresponds to variable  $x$  defined in Section 2.

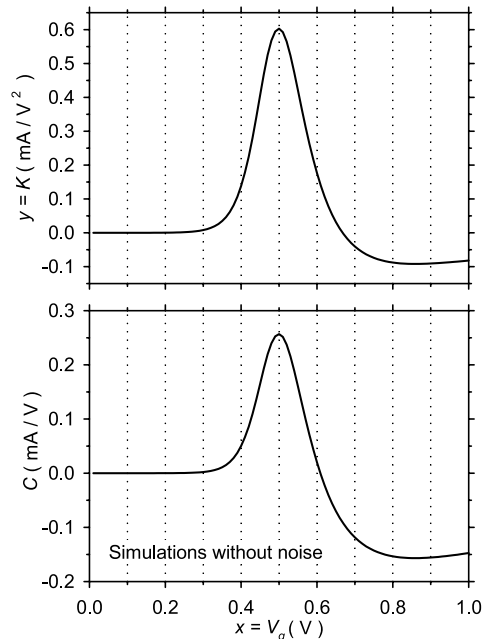


Fig. 2. (a) Simulated  $K$ - $V_g$  characteristics, obtained from  $K = d^2I_D/dV_g^2$ , for the case without noise. The variable  $K$  and  $V_g$  correspond to variables  $y$  and  $x$  defined in Section 2. (b) Corresponding Content,  $C = KV_g - \int_0^{V_g} K dV_g$ , of variable  $K$  versus  $V_g$ .

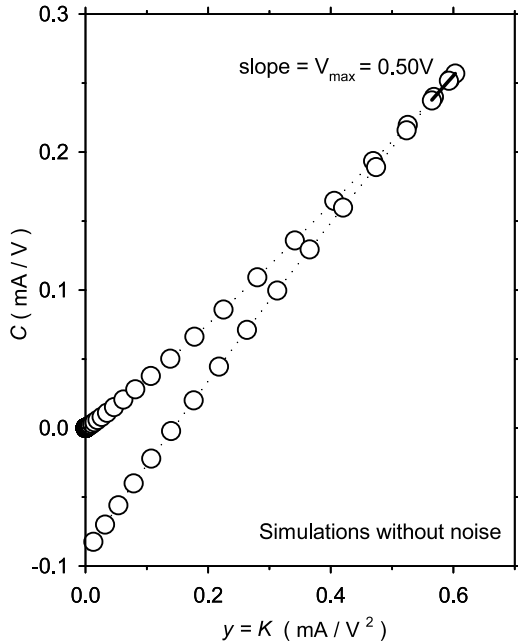


Fig. 3. Corresponding Content,  $C = KV_g - \int_0^{V_g} K dV_g$ , versus variable  $K (= y)$  for the results presented in the previous figure for the case without noise. The slope of this plot gives  $V_g (= x)$  and evaluated at the peak yields  $V_g = V_{max} (= x = x_{max})$ .

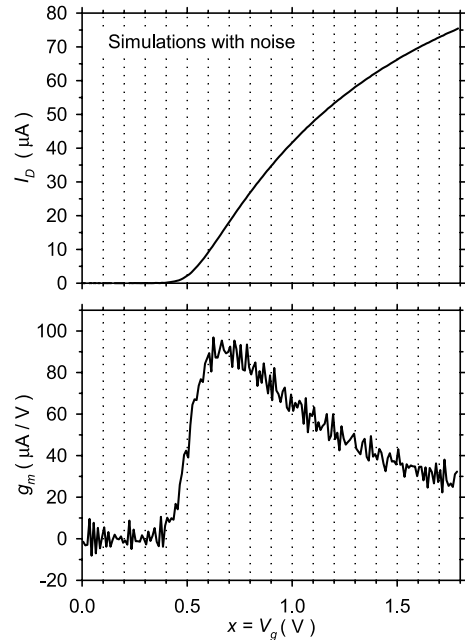


Fig. 4. (a) Simulated  $I_D-V_g$  transfer characteristics at  $V_d = 10$  mV with increments of 10 mV with an experimental noise of 0.1  $\mu A$ ; and (b) resulting transconductance obtained from  $g_m = dI_D/dV_g$ . The variable  $V_g$  corresponds to variable  $x$  defined in Section 2.

101 less case. The variable  $K$  corresponds to the variable  $y$   
 102 defined in Section 2. The plot in Fig. 2(a) represents the  
 103 function whose maximum location we wish to deter-  
 104 mine. Fig. 2(b) illustrates the Content,  $C \equiv \int_0^K V_g dK =$   
 105  $KV_g - \int_0^{V_g} K dV_g$ , versus  $V_g$ . We see in Fig. 2 that the  
 106 maxima of both functions occur at the same  $x_{max} =$   
 107  $V_{g\ max} = 0.5$  V which is the value of the threshold voltage  
 108 parameter used in the simulation.

109 Fig. 3 presents the Content but now plotted versus  
 110 variable  $K (= y)$ . The slope of this plot gives  $V_g (= x)$   
 111 which when evaluated at the peak yields  $V_g = V_{max} =$   
 112  $V_T = 0.5$  V ( $= x = x_{max}$ ). In this figure, the symbols and  
 113 dots are the simulated values and the short solid line is  
 114 the linear fit at the peak values.

#### 115 4. Application to simulated characteristics with noise

116 In order to illustrate a particular case in which the  
 117 location of the maximum slope of  $g_m$  cannot be obtained  
 118 directly, we add noise to the simulated  $I_D-V_g$  charac-  
 119 teristics presented in Fig. 1. The noise is generated using  
 120 random numbers between  $-0.05$  and  $+0.05$   $\mu A$ . Fig. 4(a)  
 121 shows the simulated  $I_D$  versus  $V_g$  characteristics with  
 122 added noise. Fig. 4(b) presents the corresponding  
 123 transconductance obtained from:  $g_m \equiv dI_D/dV_g$ . We  
 124 observe in this figure that an insignificant error in the

$I_D-V_g$  characteristics produces a large error in  $g_m-V_g$  125  
 because of the first derivative. 126

127 Fig. 5(a) illustrates the simulated  $K-V_g$  characteristics  
 128 obtained from  $K \equiv dg_m/dV_g \equiv d^2I_D/dV_g^2$  for this case  
 129 with noise. Comparing Fig. 5(a) to Fig. 2(a) we observe  
 130 that the noise has strongly concealed the maximum. Fig. 130  
 131 5(b) shows the corresponding Content of variable  $K$   
 132 versus  $V_g$ . We see in this figure that the location of the  
 133 Content maximum appears to be gone because of the  
 134 noise.

135 Fig. 6 illustrates the Content versus variable  $K (= y)$   
 136 for the results presented in the previous figure. This plot  
 137 does not present a peak, as was the case in Fig. 3, be-  
 138 cause of the high level of noise. A linear fit at high  
 139 values, above the multiple intersection region, allows to  
 140 define the straight line which matches the previous case  
 141 without noise. In this figure, the symbols and dots are  
 142 the simulated values and the solid line is the linear fit at  
 143 high values. The slope of this straight line yields  
 144  $V_g = V_{max} = 0.49$  V, which is very close to  $V_T = 0.5$  V.

#### 145 5. Application to experimental characteristics

146 In order to illustrate a real case, Fig. 7(a) shows  
 147 measured  $I_D-V_g$  characteristics of a state-of-the art bulk

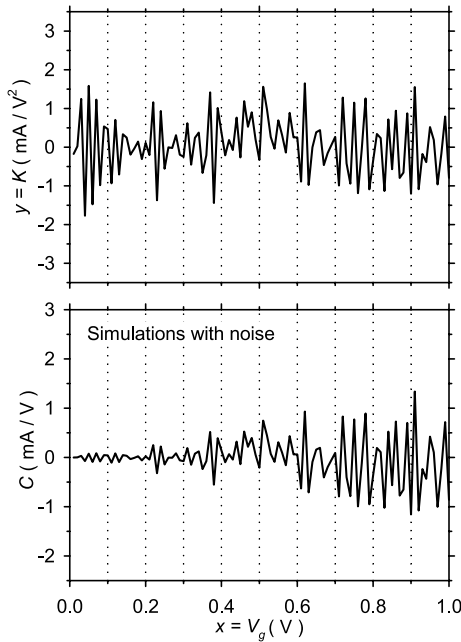


Fig. 5. (a) Simulated  $K-V_g$  characteristics, obtained from  $K = d^2 I_D / dV_g^2$ , for the case with noise. The variable  $K$  and  $V_g$  correspond to variables  $y$  and  $x$  defined in Section 2. (b) Corresponding Content,  $C = KV_g - \int_0^{V_g} K dV_g$ , of variable  $K$  versus  $V_g$ .

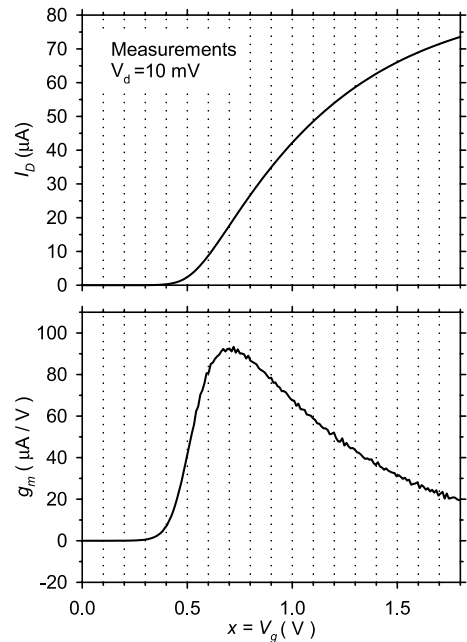


Fig. 7. (a) Measured  $I_D-V_g$  transfer characteristics at  $V_d = 10$  mV with increments of 10 mV; and (b) resulting transconductance obtained from  $g_m = dI_D / dV_g$ . The variable  $V_g$  corresponds to variable  $x$  defined in Section 2.

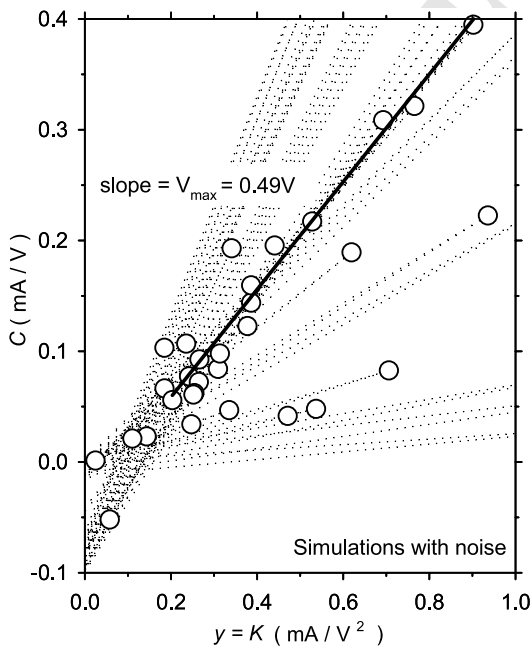


Fig. 6. Corresponding Content,  $C = KV_g - \int_0^{V_g} K dV_g$ , versus variable  $K (= y)$  for the results presented in the previous figure for the case without noise. The slope of this plot gives  $V_g (= x)$  and evaluated at the peak yields  $V_g = V_{\text{max}} (= x = x_{\text{max}})$ .

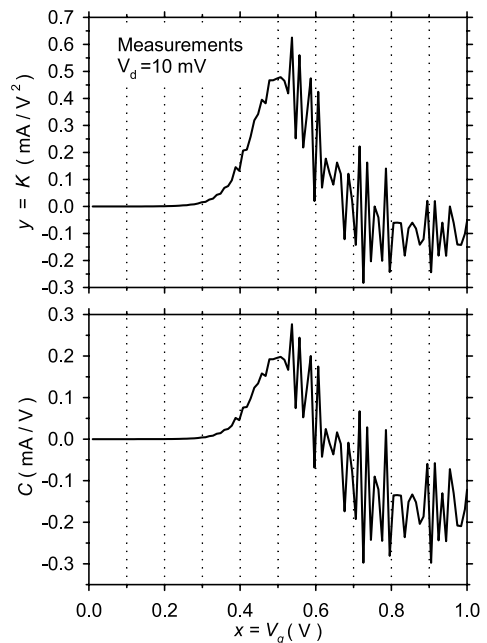


Fig. 8. (a) Simulated  $K-V_g$  characteristics, obtained from  $K = d^2 I_D / dV_g^2$ , for the measured data. The variable  $K$  and  $V_g$  correspond to variables  $y$  and  $x$  defined in Section 2. (b) Corresponding Content,  $C = KV_g - \int_0^{V_g} K dV_g$ , of variable  $K$  versus  $V_g$ .

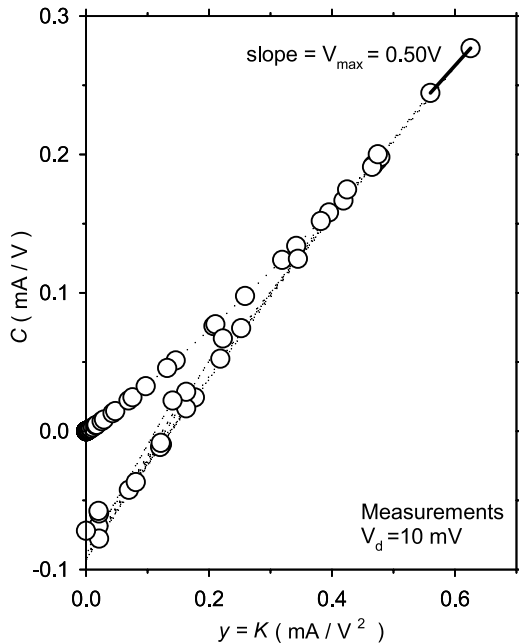


Fig. 9. (a) Corresponding Content,  $C = KV_g - \int_0^{V_g} K dV_g$ , versus variable  $K (= y)$  for the measured results presented in the previous figure. The slope of this plot gives  $V_g (= x)$  and evaluated at the peak yields  $V_g = V_{max} (= x = x_{max})$ .

148 single-crystal silicon enhancement-mode  $n$ -channel  
149 MOSFET with a  $5 \mu\text{m}$  mask channel width, a  $0.18 \mu\text{m}$   
150 mask channel length, and a  $32 \text{ \AA}$  gate oxide thickness.  
151 The corresponding transconductance is presented Fig.  
152 7(b).

153 Fig. 8(a) illustrates  $K-V_g$  characteristics obtained from  
154  $K \equiv dg_m/dV_g \equiv d^2I_D/dV_g^2$  for this experimental device.  
155 Fig. 8(b) shows the corresponding Content,  $C = KV_g -$   
156  $\int_0^{V_g} K dV_g$ , versus  $V_g$ . Notice in this figure that the maxi-  
157 mum value of  $K = d^2I_D/dV_g^2$  occurs at about  $V_g = 0.54$   
158 V due to the measurement noise present; whereas if the  
159 noise were suppressed the maximum appears to be  
160 around  $V_g = 0.50 \text{ V}$ .

161 Fig. 9 illustrates the Content versus variable  $K (= y)$   
162 for the results presented in the previous figure. In this  
163 figure, the symbols and dots are the simulated values  
164 and the solid line is a linear fit at high values above the  
165 intersection region. The slope of this linear fit yields  
166  $V_g = V_{max} = 0.50 \text{ V}$  which is a reasonable value for the  
167 threshold voltage of this device which has been studied  
168 previously [4].

## 6. Conclusions

We have presented a new method to evaluate the location of the maximum of a given function under the presence of high level of noise. This method is based on integration in order to decrease the effects of the experimental noise. This method has been verified using simulated and measured noisy MOSFET characteristics.

## References

- [1] Schroeder DK. Semiconductor material and device characterization. 2nd ed. New York: Wiley; 1998. 177-178
- [2] Liou JJ, Ortiz-Conde A, García Sánchez FJ. Analysis and design of MOSFETs: modeling, simulation and parameter extraction. New York, USA: Kluwer Academic Publishers; 1998. 179-182
- [3] Ortiz-Conde A, García Sánchez FJ, Liou JJ. An overview on parameter extraction in field effect transistors. Acta Cient Venez 2000;51:176-87. 183-185
- [4] Ortiz-Conde A, García Sánchez FJ, Liou JJ, Cerdeira A, Estrada M, Yue Y. A review of recent MOSFET threshold voltage extraction methods (Invited). Microelectron Reliab, in press. 186-189
- [5] Wong HS, White MH, Krutsick TJ, Booth RV. Modeling of transconductance degradation and extraction of threshold voltage in thin oxide MOSFET's. Solid-State Electron 1987;30:953. 190-193
- [6] García Sánchez FJ, Ortiz-Conde A, Mercato GD, Salcedo JA, Liou JJ, Yue Y. New simple procedure to determine the threshold voltage of MOSFETs. Solid-State Electron 2000;44:673-5. 194-197
- [7] García Sánchez FJ, Ortiz-Conde A, De Mercato G, Liou JJ. Parameter extraction and signal processing using potential functions. Univ Cienc Tecnol 2000;4:123-36. 198-200
- [8] García Sánchez FJ, Ortiz-Conde A, De Mercato G, Liou JJ, Recht L. Eliminating parasitic resistances in parameter extraction of semiconductor device models. In: Proc. First IEEE Int. Caracas Conf. Dev. Cir. Sys. 1995; Caracas, Venezuela, p. 298. 201-203
- [9] Cerdeira A, Estrada M, Quintero R, Flandre D, Ortiz-Conde A, García Sánchez FJ. New method for determination of harmonic distortion in SOI FD transistors. Solid-State Electron 2002;46:103-8. 204-209
- [10] Fjeldly TA, Ytterdal T, Shur M. Introduction to modeling and circuit simulation. New York: Wiley; 1998. Available from: [www.aimspice.com](http://www.aimspice.com). 210-212
- [11] Chua LO. Stationary principles and potential functions for nonlinear networks. J Franklin Inst 1973;296:91-114. 213-214
- [12] García Sánchez FJ, Ortiz-Conde A, Cerdeira A, Estrada M, Flandre D, Liou JJ. A method to extract mobility degradation and total series resistance of fully-depleted SOI MOSFETs. IEEE Trans Electron Dev 2002;49:82-8. 215-218

169

170  
171  
172  
173  
174  
175

176

177  
178  
179  
180  
181  
182  
183  
184  
185  
186  
187  
188  
189  
190  
191  
192  
193  
194  
195  
196  
197  
198  
199  
200  
201  
202  
203  
204  
205  
206  
207  
208  
209  
210  
211  
212  
213  
214  
215  
216  
217  
218